HNPS Advances in Nuclear Physics

Large Sample Neutron Activation Analysis for Cultural Heritage Studies

T. Vasilopoulou, F. Tzika, I. E. Stamatelatos

Large Sample Neutron Activation Analysis for Cultural Heritage Studies

T. Vasilopoulou[1, 2], F Tzika[1] and I. E. Stamatelatos[1]

[1]*Institute of Nuclear Technology - Radiation Protection, NCSR 'Demokritos', 15310 Aghia Paraskevi, Athens, Greece*

[2]*School of Applied Mathematical and Physical Science, National Technical University of Athens, 15780 Athens, Greece*

_____

Abstract

Large Sample Neutron Activation Analysis (LSNAA) is a non-destructive, multi-element analysis technique with a broad range of scientific and technological applications. Since both neutrons and gamma rays have penetration depths of the order of several centimeters within materials, depending on their energy and sample material properties, LSNAA enables non-destructive compositional analysis of the inner structure of large volume samples (up to several litters in volume). In this work, applications of LSNAA in cultural heritage studies are presented and the unique capabilities of the technique for bulk sample elemental analysis of precious and archaeological objects that need to be preserved intact and cannot be damaged for sampling purposes are discussed.

Keywords: Neutron Activation Analysis, Large Sample, Cultural Heritage Studies

_____

1. Introduction

Neutron Activation Analysis (NAA) is a non-destructive, multi-element analysis technique with excellent sensitivity, great accuracy, precision and linearity that has found a broad range of applications in several fields of science and technology, including archaeology [1]. In conventional NAA, the mass of analyzed samples is in the range of milligrams to grams (or of a few µl to ml in volume), representing only a small portion of the bulk material. Nevertheless, there are applications, such as authenticity and provenance studies, where the analyzed objects need to be preserved intact or representative sampling from the bulk material cannot be performed. Furthermore, in the case of heterogeneous materials, which are often met in archaeological studies, representative sampling is often a very difficult or even impossible task [2].

Large Sample Neutron Activation Analysis (LSNAA) enables non-destructive analysis of bulk objects, up to several liters in volume, as a whole. Therefore, responds to the requirement for a non-invasive multi-elemental technique capable to analyze large samples that are too precious to remove small parts from, such as archaeological objects and artifacts [3, 4].

In LSNAA the sample is irradiated at a research reactor graphite thermal neutron column and subsequently transferred to a gamma ray spectrometry system to be counted either as a whole [5] or using a scanning geometry counting configuration [6]. Analysis of the acquired gamma spectra allows the evaluation of the elemental composition of the sample. Corrections are required for self-shielding of the activating neutrons [7, 8], self-absorption of gamma rays [9], heterogeneity of the sample [10, 11] and geometric factor during gamma counting [12]. K_0 and internal mono-standard based calibration techniques for LSNAA have been presented [13, 14].

In the present work, LSNAA of two large ceramic samples representing museum objects is presented. The appropriate neutron self-shielding and gamma ray detection efficiency calibration factors were derived using the Monte Carlo method. The results of this work provide a nuclear analytical procedure for bulk sample elemental analysis of precious and archaeological objects that need to be preserved intact and reveal the novel research opportunities arising from the direct analysis of large volume samples as a whole in cultural heritage studies.

2. Experimental

Samples

Two large samples were analyzed. The first one was a commercially purchased handmade ceramic vase representing a Greek archaeological museum piece. The outer dimensions of the vase were 11.50 cm in diameter (at maximum) and 15.60 cm in height. The average wall thickness was 0.43 cm and its mass was 376 gr. It is noted that the external surface of the vase was painted by acrylic colors.

The second analyzed item was a Peruvian pottery object, replicate of a Pre-Columbian archaeological artifact [15]. It was an animal-shaped ceramic bottle of 25.70 cm in height and 9.60 cm in maximum diameter. The average wall thickness was 0.70 cm and its mass was 780 gr. The bottle was prepared by IPEN (Peru) for the purposes of an international LSNAA inter-comparison study organized by IAEA.

Irradiation

In both cases, the experimental procedures were performed at the facilities of Reactor Institute Delft, Delft University of Technology (The Netherlands). Neutron irradiation was performed at the Big Sample Neutron Irradiation System (BISNIS) installed at Hoger Onderwijs Reactor graphite thermal neutron column [16]. BISNIS provides a moderated neutron flux of 5×10^8 cm$^{-2} \cdot$s^{-1}. The irradiation time was 12 h for the Greek vase and 48 h for the Peruvian bottle. During irradiation zinc flux monitors were positioned on the surface of each sample.

Gamma-ray counting

Measurement of emitted gamma rays was performed using a HPGe detector based spectrometry system. The gamma ray detection system is described in detail elsewhere [17]. The detector consisted of a HPGe crystal of 96% relative efficiency, 1.82 keV energy resolution at the 1332 keV ^{60}Co photo-peak and peak to Compton ratio of 97:1. Activation gamma ray spectra were measured in different decay times after irradiation. During measurement the bulk sample was rotated around its vertical axis to minimize axial non-uniformity of activation. In each case, the distance from the detector surface to the axis of rotation was 20 cm. The acquired activation spectra were corrected with the corresponding gamma ray background spectra. Spectrum analysis was performed using Gamma Vision software.

Monte Carlo simulations

Monte Carlo code MCNP, version 5 [18], was used in order to model the neutron irradiation and gamma counting configurations and derive the required LSNAA correction factors. Since these factors depend on the geometry and material of the sample, a close approximation of the studied object was required. Thus, in the case of the animal-shaped Peruvian bottle, CT scan was employed to provide complementary information on the significantly complicated geometry. CT scan was performed using an Aquilion Toshiba 64 series CT medical system and the tomography data obtained enabled an accurate representation of the sample in MCNP input files. Moreover, the graphite pile, irradiation container and HPGe detector were modeled in detail. Cross section data from the Evaluated Nuclear Data File (ENDF) system were used for the computations [19]. The analyzed items and the corresponding MCNP sample geometry models are shown in Figure 1.
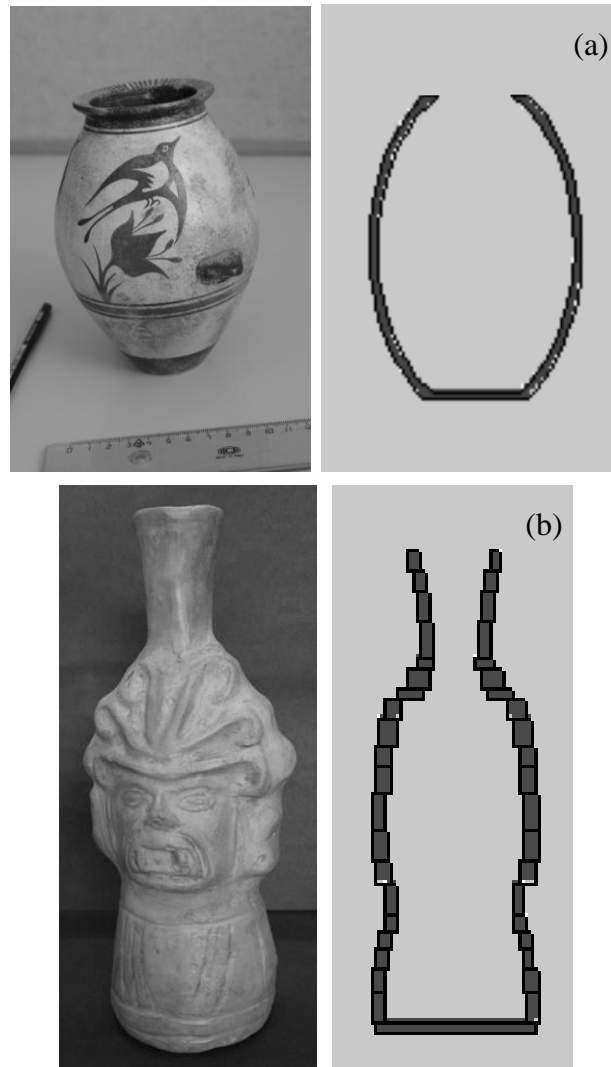

Fig. 1 Picture of the analyzed item and the corresponding MCNP sample geometry model of (a) the Greek vase and (b) the Peruvian bottle

Simulations were performed assuming thermal neutrons incident on the surface of the graphite pile. Thermal fluxes were predicted using track length estimates of neutron flux, in units of cm^{-2} per source neutron. The neutron self-shielding correction factor, f_n, was calculated as the ratio of the average predicted thermal neutron flux throughout the volume of the ceramic sample to the average predicted thermal neutron flux over its external surface. The activating neutron flux was derived by combining the experimentally determined thermal neutron flux on the surface of the sample as measured by zinc monitors and the MCNP predicted neutron self-shielding correction factor.

The HPGe detector full energy peak efficiency (FEPE) for the voluminous source geometry configuration was calculated using the efficiency transfer method on the basis of the FEPE measured for a reference point source [20]. MCNP code was used to predict FEPE for the reference point source at 20 cm distance from the detector (at the geometrical centre of the ceramic sample) and for the actual ceramic volume source configuration in order to derive the efficiency transfer factor, for each sample. Pulse height tally was used to predict the detector's response in terms of energy deposited in the active volume of the crystal in the specified energy bin and thus estimate the absolute FEPE of the detector.

3. Results and discussion

Correction factors
Placement of the large sample within the graphite pile resulted in a perturbation of the thermal neutron field. The MCNP predicted neutron self-shielding correction factors, f_n, the average thermal neutron fluence rate measured by the zinc monitors on the sample surface, $\Phi_{S, exp}$, and the derived average thermal neutron fluence rates over the sample volume, Φ_V, for the two large samples considered are shown in Table 1.

Sample	f_n	$\Phi_{S, exp}$ ($\times 10^8$ $cm^{-2}s^{-1}$)	Φ_V ($\times 10^8$ $cm^{-2}s^{-1}$)
Greek vase	0.98 ± 0.02	4.18 ± 0.23	4.10 ± 0.24
Peruvian bottle	0.96 ± 0.01	3.91 ± 0.33	3.73 ± 0.33

Table 1. Predicted neutron self-shielding correction factors, average measured surface neutron fluence rates and derived average fluence rates over the sample volume for the two ceramic samples studied

The MCNP calculated FEPE curves for the point and the actual volume sources over the photon energy range from 100 to 1600 keV are shown in Figure 2. The corresponding efficiency transfer functions (f_γ) from point to volume source geometries, defined as the ratio of FEPE for the volume source to FEPE for the reference point source, are also plotted in this Figure. As it can be observed, f_γ increases with energy, for both samples studied. This result is attributed to the decrease in photon attenuation within the ceramic material with increasing photon energy.
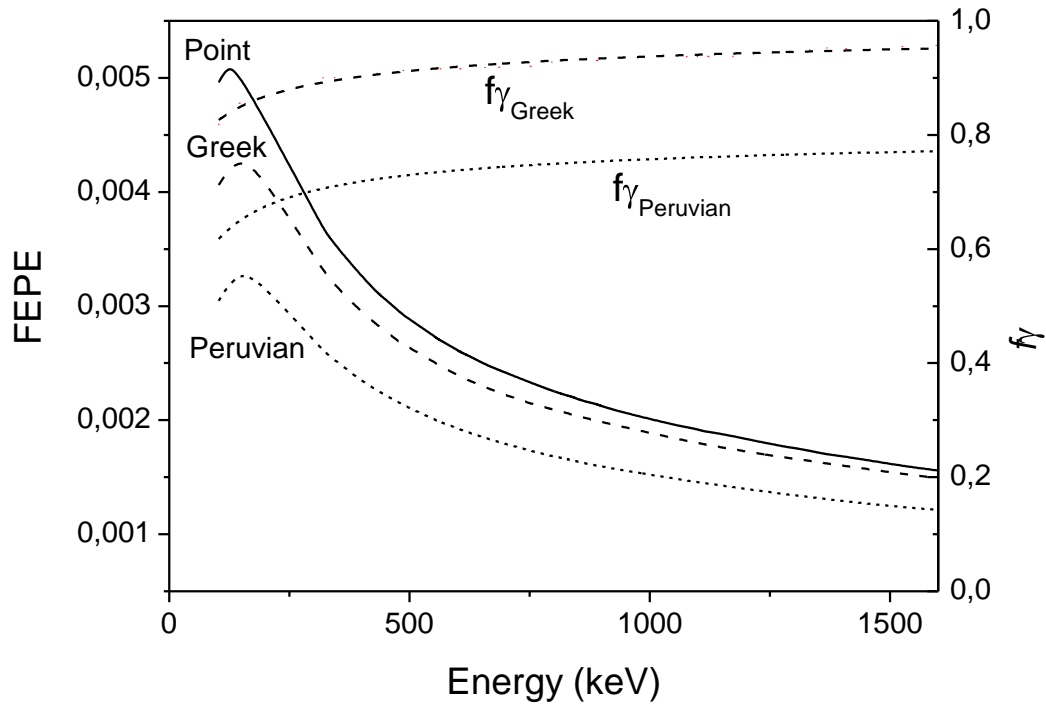
Fig. 2. Predicted FEPE for the point and volume sources and the calculated efficiency transfer factors (f_γ) as a function of photon energy for the two large samples studied

The correction factors depend on material, size and shape of the large sample itself and are sample and facility specific. From the calculated f_n and f_γ factors (Table 1 and Fig. 2) it is evident that for the ceramic samples examined in this study it is the gamma correction which is the significant.

Elemental analysis

Table 2 shows the elemental concentration results derived by LSNAA along with their standard uncertainties for the two large samples considered. It is noted that the reported combined uncertainties include all identified contributing sources related to nuclear data, experimental procedure and simulations. These include uncertainties in cross section data, measured neutron fluence rate, gamma ray counting and Monte Carlo computations.

In the case of the Greek ceramic vase, the LSNAA results were compared against values obtained by Instrumental Neutron Activation Analysis (INAA) of small samples, considered as reference values [21]. The ratios of LSNAA to INAA elemental concentration are shown in Table 3. As it can be seen, the concentration ratios were within 0.7 and 1.3, for all elements, indicating a reasonably good agreement between large sample and small sample neutron activation analysis results.

Element	Greek vase LSNAA concentration (mg/kg)	Peruvian bottle LSNAA concentration (mg/kg)
Sm	3.61 ± 0.23	3.48 ± 0.21
Sc	17.48 ± 0.95	16.60 ± 0.88
Cr	397.84 ± 22.76	27.33 ± 3.99
Fe	49833 ± 3361	36680 ± 2494
Co	32.05 ± 1.98	15.10 ± 0.85
Yb	2.26 ± 0.50	3.28 ± 0.47
As	8.44 ± 1.40	31.27 ± 3.86
Cs	7.05 ± 0.91	11.64 ± 1.43
La	28.78 ± 1.55	19.55 ± 1.03
Sb	0.64 ± 0.08	4.33 ± 0.29
Eu	0.80 ± 0.19	-
Ce	40.00 ± 4.57	-
W	1.68 ± 0.45	-
Ca	70039 ± 10112	-
Rb	139.88 ± 22.40	-
K	-	17240 ± 1104
Ga	-	17.70 ± 5.24

Table 2. LSNAA elemental concentrations along with their standard uncertainties for the two large samples

Element	Ratio LSNAA/Reference
Eu	0.70 ± 0.17
Sm	0.75 ± 0.05
Ce	0.76 ± 0.09
Sc	0.86 ± 0.05
Cr	0.86 ± 0.05
Fe	0.89 ± 0.06
Co	0.90 ± 0.06
W	0.96 ± 0.28
Ca	0.99 ± 0.15
Yb	0.99 ± 0.22
As	1.01 ± 0.17
Cs	1.03 ± 0.14
La	1.05 ± 0.06
Sb	1.20 ± 0.18
Rb	1.27 ± 0.21

Table 3. Ratio of LSNAA to reference concentration values per studied element for the Greek ceramic vase

The results presented in Tables 2 & 3 demonstrate the feasibility of performing non-destructive whole-object analysis of valuable ceramic pieces. Moreover, it is shown that a satisfactory agreement was observed between LSNAA and reference values, confirming that LSNAA is a powerful analytical tool with unique applications in cultural heritage studies.

Indeed, LSNAA has been proven particularly useful in provenance and authentication studies, where compositional profiles of individual artifacts and source materials are used in order to trace the artifacts to their place of origin. Examples of the application of the technique include provenance studies of Brazilian Tupi-Guarani tradition pottery [22], analysis of large and non-standard geometry archaeological samples [23], compositional studies on ancient pottery samples obtained from Buddhist sites of Andhra Pradesh in India [24] as well as authenticity identification of intact ancient Chinese porcelain ware [25].

4. Conclusions

In the present work, LSNAA was used for the analysis of two large ceramic samples representing museum objects. The required corrections for thermal neutron self-shielding during sample irradiation and γ-ray detection efficiency for the volume source during counting were derived using the Monte Carlo method enabling precise simulation of the complex large sample, irradiation facility and gamma ray detector configurations. Furthermore, a satisfactory agreement was observed when LSNAA results were compared against reference values, derived by INAA technique.

The results of this study demonstrated the feasibility of performing LSNAA to bulk ceramic items (as a whole) and therefore contribute to the requirement for developing validated nuclear analytical procedures for non-destructive, multi-element bulk sample analysis of precious artifacts and archaeological objects that need to be preserved intact and cannot be damaged for sampling purposes. Moreover, the unique advantages and the new possibilities arising from the direct analysis of voluminous samples have been presented. The ability to analyze whole objects distinguishes LSNAA among the analytical techniques since other established non-destructive methods (such as X-ray fluorescence analysis or analytical techniques based on charged particle irradiation-PIXE) can only analyze superficial layers of the sample and therefore provide limited information over the whole volume of the object. Moreover, LSNAA is not affected by post-depositional elemental alterations [26] since the analytical information is provided from the whole volume of the bulk object and not only from the surface layers of the material.

References

[1]   R. J. Speakman, M.D. Glascock, Archaeometry 49 (2007) 179-183

[2]   International Atomic Energy Agency, Report of the technical meeting on LSNAA using low flux irradiation facilities, IAEA, Vienna, Austria, 7-11 November 2005

[3]   International Atomic Energy Agency, Report of the 1st RCM on Application of LSNAA for inhomogeneous bulk archaeological samples and bulk objects, IAEA, Vienna, Austria, 19-23 January 2009

[4]   I. E. Stamatelatos, F. Tzika, Annali di Chimica 97 (2007) 505-512

[5]   R. M. W. Overwater, P. Bode, J. J. M. De Goeij, J. E. Hoogenboom, Anal. Chem. 68 (1996) 341-348

[6]   M. Blaauw, H. W. Baas, M. Donze, Nucl. Inst. Meth. In Phys. Research A 505 (2003) 512-516

[7]   F. Tzika, I. E. Stamatelatos, Nucl. Inst. Meth. In Phys. Research B 213 (2004) 177-181

[8]   I. H. Degenaar, M. Blaauw, J. J. M. De Goeij, J. Radioanal. Nucl. Chem. 257 (2003) 467-470

[9]   F. Tzika, I. E. Stamatelatos, J. Kalef-Ezra, P. Bode, Nukleonika, 49 (2004) 115-121

[10]   R. M. W. Overwater, P. Bode, Appl. Radiat. Isotop. 49 (1998) 967-976

[11]   F. Tzika, I. E. Stamatelatos, J. Kalef-Ezra, J. Radioanal. Nucl. Chem. 271 (2007) 233-240

[12]   R. M. W. Overwater, P. Bode, J. J. M. De Goeij, Nucl. Inst. Meth. In Phys. Research A 324 (1993) 209-218

[13]   M. Blaaw, J. Radioanal. Nucl. Chem. 220 (1997) 233-235

[14]   A. G. C. Nair, R. Acharya, K. Sudarshan, S. Gangotra, A. V. R. Reddy, S. B. Manohar, A. Goswami, Anal. Chem. 75 (2003) 4868-4874

[15]   E. Montoya, 2nd RCM of the IAEA CRP on Application of LSNAA for Inhomogeneous Bulk Archaeological Samples and Bulk objects, Delft, The Netherlands, 17-21 May 2010

[16]   R. M. W. Overwater, J. E. Hoogenboom, Nucl. Sc. Eng. 117 (1994) 141-157

[17]   P. Bode, R. M. W. Overwater, J. J. M. De Goeij, J. Radioanal. Nucl. Chem. 216 1 (1997) 5-11

[18]   X-5 Monte Carlo Team, MCNP - A General Monte Carlo N-Particle Transport Code, Version 5, LA-UR-03-1987, April 2003

[19]   P. F. Rose, Compiler and Editor, ENDF-201, ENDF/B-VI Summary Documentation, BNL-NCS-17541, Brookhaven National Laboratory, October 1991

[20]   F. Piton, M. C. Lepy, M. M. Be, J. Plagnard, Appl. Radiat. Isotop. 52 (2000) 791-795

[21]   I. E. Stamatelatos, F. Tzika, T. Vasilopoulou, M. J. J. Koster-Ammerlaan, J. Radioanal. Nucl. Chem. 283 (2010) 735–740

[22]   G. L. O. Faria, M. Â. B. C. Menezes, L. Ribeiro, C. Jacome, International Nuclear Atlantic Conference - INAC 2009, Rio de Janeiro, Brazil, September 27 to October 2, 2009

[23]   K. Sueki, Y. Oura, W. Sato, H. Nakahara, T. Tomizawa, J. Radioanal. Nucl. Chem. 234 (1998) 27-31

[24]   K. B. Dasari, R. Acharya, K. K. Swain, N. Lakshmana Das, A. V. R. Reddy, J. Radioanal. Nucl. Chem. 286 (2010) 525–531

[25]   F. Songlin, F. Xiangqian, Y. Lingtong, L. Li, 2nd RCM of the IAEA CRP on Application of LSNAA for Inhomogeneous Bulk Archaeological Samples and Bulk objects, Delft, The Netherlands, 17-21 May 2010

[26]   A. Schwedt, H. Momusen, N. Zacharias, Archaeometry 46 (2004) 85-101